TELKOMNIKA, Vol.16, No.1, February 2018, pp. 69~76
ISSN: 1693-6930, accredited **A** by DIKTI, Decree No: 58/DIKTI/Kep/2013
DOI: 10.12928/TELKOMNIKA.v16i1.6004

NO_2 Gas Sensing Properties of Carbon Films Fabricated by Arc Discharge Methane Decomposition Technique

Elnaz Akbari[1], Zolkafle Buntat*[2], Syed Muhamad Zafar Iqbal[3], Zulkifli Azman[4], Norain Sahari[5], Zainuddin Nawawi[6], Muhammad Irfan Jambak[7], Muhammad Abu Bakar Sidik[8]
[1,2,3,4,5]Institute of High Voltage & High Current, Faculty of Electrical Engineering, Universiti Teknologi Malaysia, Johor Bahru, 81310 Malaysia
[6,7,8]Department of Electrical Engineering, Faculty of Engineering, Universitas Sriwijaya, Prabumulih KM 32, Indralaya Ogan Ilir, 30662 South Sumatera, Indonesia.
*Corresponding author: zolkafle@utm.my, abubakar@unsri.ac.id

Abstract

In this work, a set of experiments has been conducted using arc discharge Methane decomposition attempting to obtain carbonaceous materials (C-strands) formed between graphite electrodes. The current-voltage (I-V) characteristics of the fabricated C-strands have been investigated in the presence and absence of two different gases, NO_2 and CO_2. The results reveal that the current passing through the carbon films increases when the concentrations of gases are increased from 200 to 800 ppm. This phenomenon is a result of conductance changes and can be employed in sensing applications such as gas sensors.

Keywords: *Carbonaceous materials, gas sensing, methane arc discharge decomposition, I-V characteristics*

1. Introduction

A novel method for the fabrication of a carbon based material implementing high voltage AC arc discharge has been attempted to design and develop. This carbon based material is intended to be utilized in an electric circuit to build up a gas sensing mechanism [1-5]. By applying a high AC voltage to the graphite electrodes employed in the experimental set up, an arc ignites between the electrodes as the gas between them is ionized. This arc is employed in the methane decomposition process which results in carbon strands that we intend to fabricate. Pure methane in atmospheric pressure is passed over the electrodes inside a Pyrex glass tube chamber where the carbon strand fabrication process takes place [6], [7]. Once the arc ignites between the graphite electrodes, the methane gas starts to decompose to its constituent species. At the end of this process a fine soot of carbonaceous material remains between the two electrodes. The material produced this way is then checked through high resolution optical microscopy as well as scan electron microscopy (SEM) to observe the material physical and structural characteristics. Once the carbon strands are grown, the measurement process is carried out.

2. Experimental Details

An illustration of the complete experimental setup assembly employed in high voltage AC arc discharge generation is provided in Figure 1. Methane gas by using a gas flow meter at a constant flow of 0.2-1.0 standard litter per minute (SLPM) was passed through the chamber. The chamber is connected between gas cylinder and flow controller. The material which is used in chamber fabrication is Pyrex glass. A pressure regulator has been used to ensure the gas flow has the atmospheric pressure. The Neon transformer was implemented to increase the voltage to kilovolt and it is necessary for decomposition process. For the purpose of high voltage monitoring a high voltage probe was used to measure and record the signals via

Received August 20, 2017; Revised December 15, 2017; Accepted January 5, 2018

oscilloscope. The scan electron microscope and high resolution optical microscope were provided for the structural morphology of carbon film.

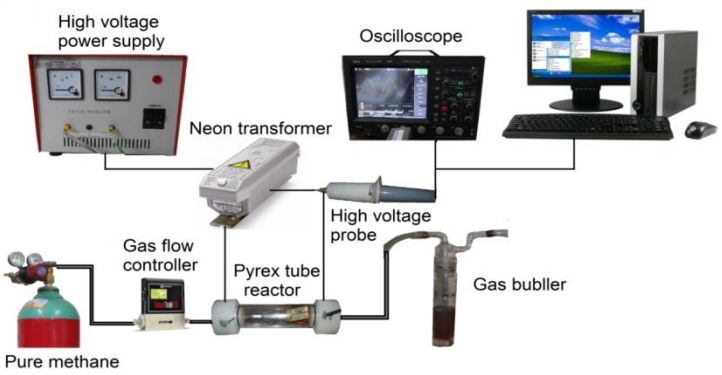

Figure 1. Experimental setup of arc discharge methane decomposition process

The parameters of this process are tabulated in Table 1.

Table 1. The operating factors in carbon film fabrication

Factors	Rate
Voltage	1-26 kV
Frequency	50 Hz
Gas type	Pure Methane (99.99%)
Temperature	At Room Environment
Pressure	Atmospheric
Rate of flow	0.2-1.0 SLPM

2.1. Fabricated C-Strands

Three different configurations of graphite electrodes were fixed on a PCB board and used for sample growth. These configurations are plane-to-plane (PTP), tip-to-plane (TTP) and tip-to-tip (TTT). The methane decomposition and carbon deposition process results in a minute soot of carbon atoms formed along the axis of the aligned electrodes. The fact that the material fabricated in this process is made of carbon is checked through Optical Emission Spectroscopy, as will be explained in the following section. Once the arc discharge is initiated, methane decomposition starts causing the resultant carbon atoms to deposit and stack up between the two electrodes creating a conductive bridge. The C-strand developed in the experiment was also inspected using optical microscope. Figures 2(a, b) show the corresponding images obtained from high resolution optical microscopy at magnification X16. Figure 2(a) illustrates the PTP and Figure 2(b) shows the TTT electrode configurations.

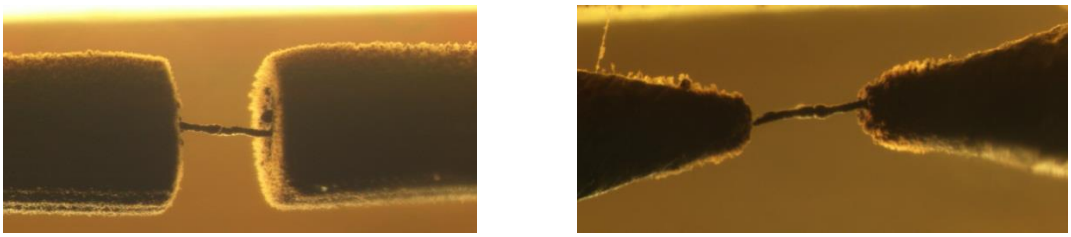

(a) (b)

Figure 2. Fabricated C-strand at magnification of X16 (a) PTP, (b) TTT

2.2. Optical Emission Spectroscopy (OES) Setup

In this study, OES was implemented to make sure that the material produced during the methane decomposition is made of carbon. An illustration of the general configuration in which the devices have been connected and utilized in the experiment has been provided in Figure 3. As shown, the probe at the tip of the fiber optical cable has been in close contact with the Pyrex chamber and the spectrometer is connected to a computer to record the spectra emitted during the carbon growth state enabling us to capture the spectra of the sparks ignited during the process and compare them with those in other works [8-10]. This will allow assuring that the material deposited between the electrodes is carbonaceous.

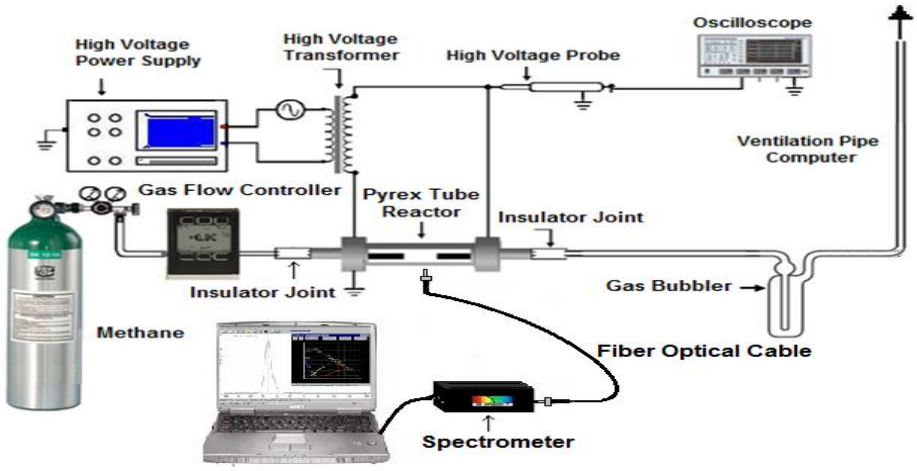

Figure 3. Setup for optical emission spectroscopy

The range of wavelength (385-750 nm) was measured by the optical emission spectroscopy and the MATLAB software was used for sketching these data. As shown in Figure 4 and figure 5 the three developed peaks are hydrogen Hα=657.33 nm, CH=397 and 431 nm, and C2=516.75 [11, 12].

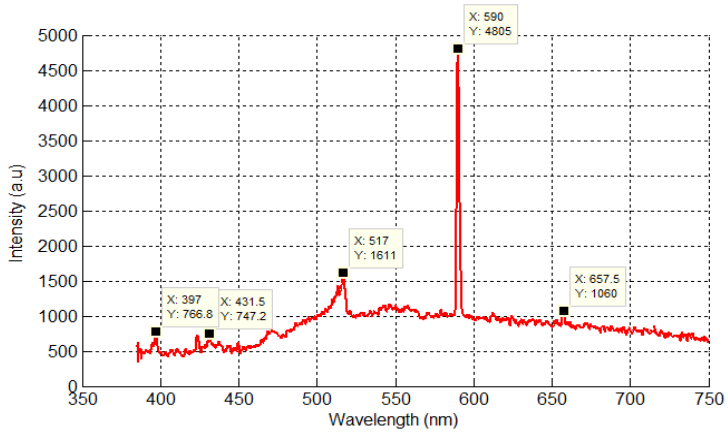

Figure 4. Optical emission spectroscopy of methane during decomposition process

The ranges of the peaks are tabulated in Table 2.

Table 2. Types of methane gas

Gas typs	Wavelength (nm)	Energy (eV)
C2	516.75	3.4
	590	-
Hα	657.5	3.3
CH	397	-
	431.4	2.9

2.3. Scan Electron Microscopy

The samples obtained at the end of the decomposition are then inspected with scanning electron microscope (SEM)analysis [13]. The images which are provided by SEM are shown in Figures 6(a) and 6(b).

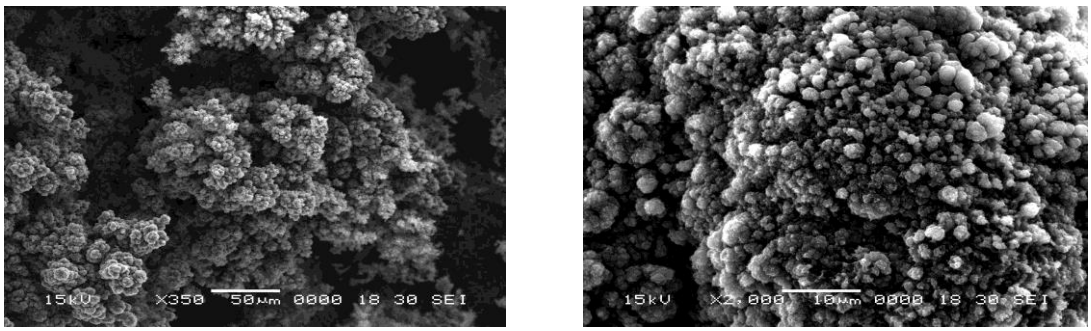

(a) (b)

Figure 6. SEM image of a sample, imaging mode a) X350 at 15 kV; b) X2000 at 15 kV

Between a wide range of carbon allotropes, just graphite, graphene, and carbon nanotubes, has electrical conductivity. The fabricated carbon film material can belong to one of the graphitized materials due to the grown carbon in this study also show conducting behaviour [14-16]

2.4. Electrical Characterization of the Grown C-Strand

The current-voltage characteristics of the C-strands obtained were tested and evaluated in order to assess their potential ability to replace the channel in gas sensors. Applying a DC voltage to the C-strands in successive time periods after the growth, the corresponding currents passing through the conductive channel has been measured and recorded. The schematic of the electrical structure is shown in Figure 7. The current was measured and recorded by Ampermeter in Figures 8(a,b,c) and Figure 9(a,b,c), when the voltage was increased from 0-10 volts. The growing configuration data including the electrode gaps, growing voltages as well as the growing time has been tabulated in Table 3.

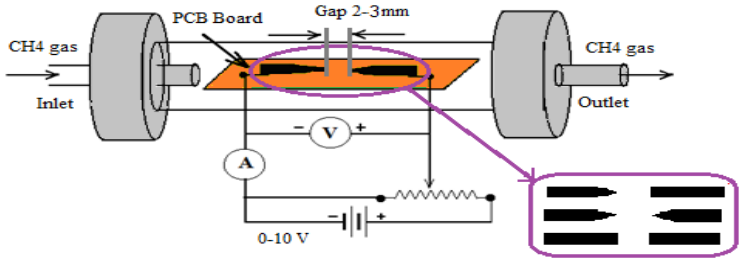

Figure 7. Electrical measurement set up for the C-strands grown between different electrode configurations

Table 3. Effect of electrode configurations on the growth of C-strands

Configuration of Electods		Gap (mm)	High Voltage (kV)	Growing Time (s)
Set A	PTP	0.2	18.9	9.39
	PTP	0.3	25.6	11.77
Set B	TTT	0.2	17.1	12.20
	TTT	0.3	23.5	8.28
Set C	TTP	0.2	15.3	12.20
	TTP	0.3	21.4	13.07

3. Experimental Results from the Electrical Measurements

3.1. Under CO_2 Exposure

The changes in the current passing through the C-strands as a result of voltage alterations were measured and recorded. The measurements were carried out under the exposure to gas immediately after growth and also several minutes after growth for TTT configuration with D=2mm in the presence of CO_2 with concentrations of 200, 400, and 800 ppm. The voltage was increased from zero to 5 Volts and the corresponding currents passing through the circuit were recorded using a micro-Ampermeter. The current-voltage readings are provided in Figure 8(a to e).

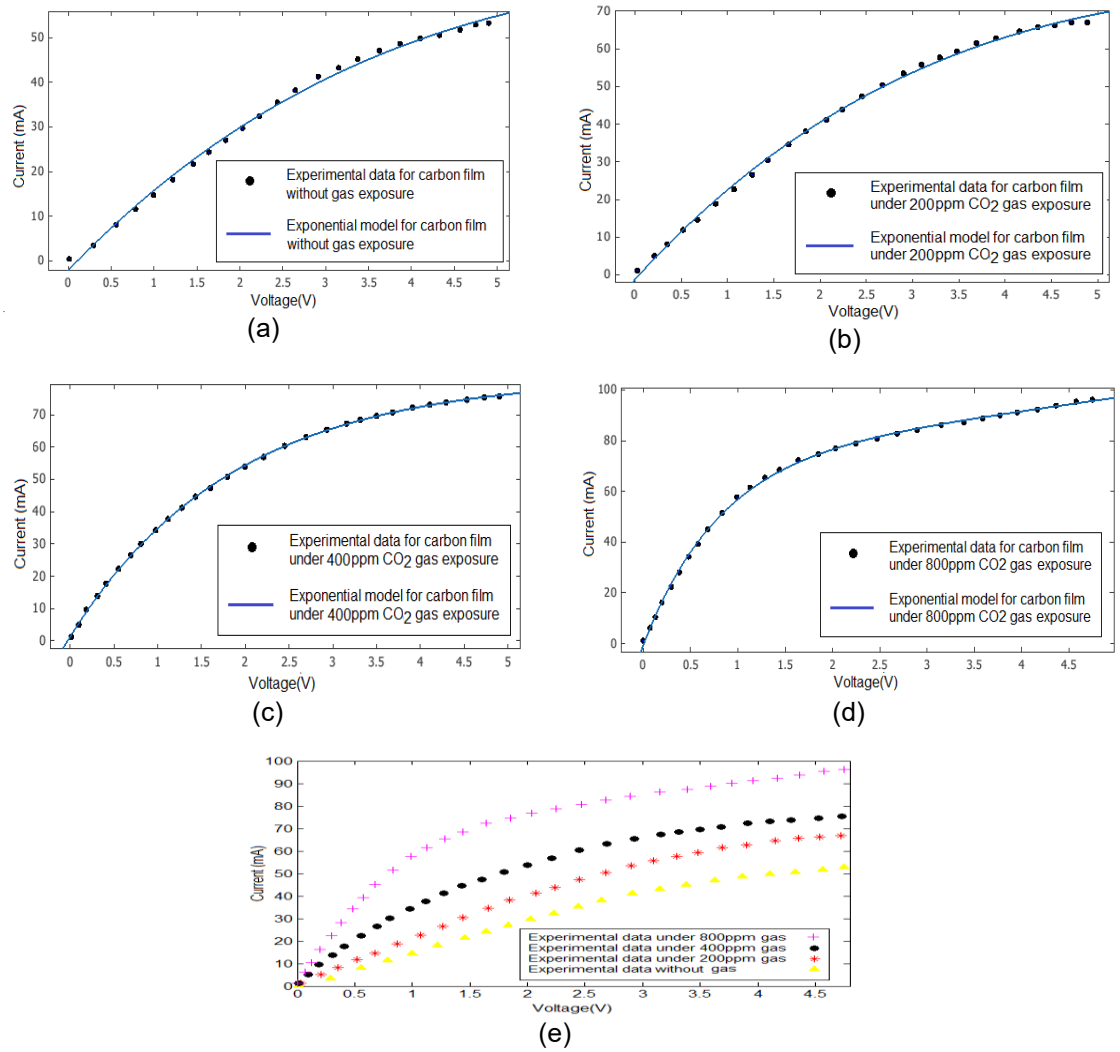

Figure 8. I-V characteristics of carbon film a) before CO_2 exposure, b) under 200 ppm gas; c) under 400 ppm gas; d) under 800 ppm gas; e) comparing all (a) to (d)

3.2. Under NO_2 Exposure

As can be seen in Figure (9), when the C-strand is exposed to NO_2 gas, according to the chemical reaction between carbon film and NO_2 gas molecules, carbon experiences a change in the velocity of its carriers which can in turn induce alterations in the current and channel voltage. In other terms, the electron exchange between the gas and the surface of the carbon creates new carriers which change the conductivity of electrons.

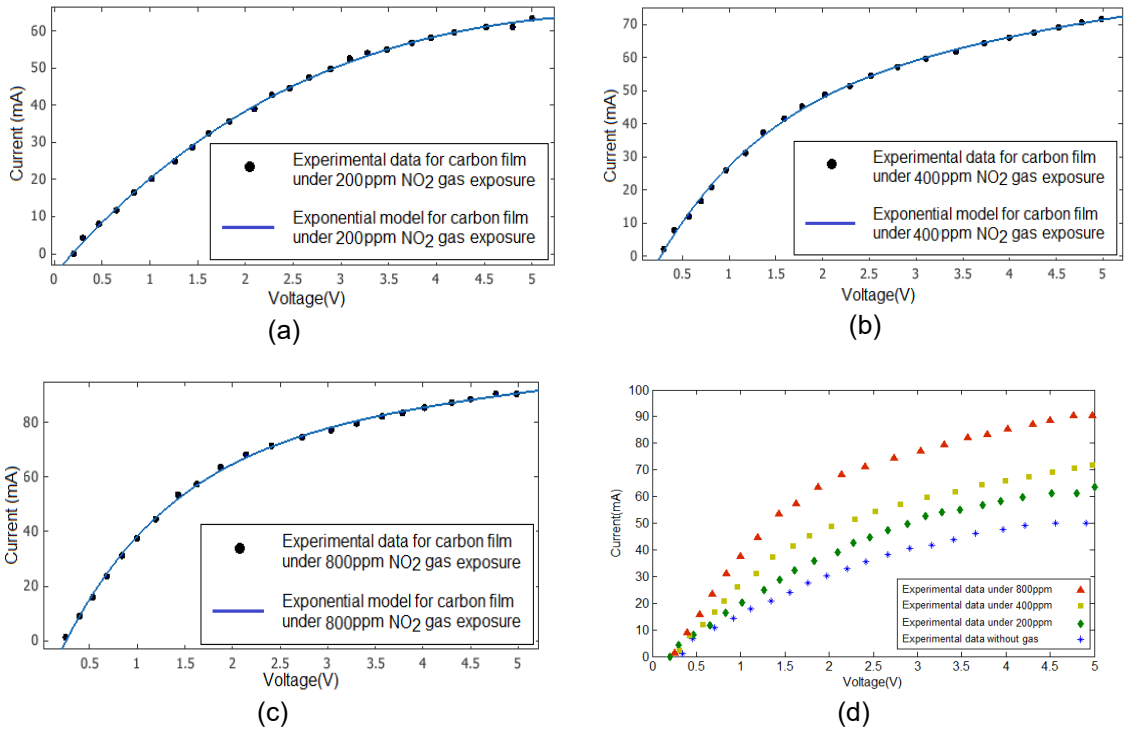

Figure 9. Current-voltage characteristics under NO_2 gas exposure, 200 ppm, b) 400 ppm, c) 800 ppm, e) all data comparison

Under the gas exposure (200 ppm to 800 ppm), by carrier concentration increment the current was further increased. An increase in the current can be associated to the charge transfer between carbon film and NO_2 molecules. This phenomenon is also known as chemical doping by gas molecules. Exchange of electrons due to absorption of NO_2 gas molecules on the carbon film causing a modification of the electrical conductance in the carbon film which is the basic concept for high sensitively molecular sensor. When the gas concentration increased from 200pp, to 800ppm the I-V characteristics increased as well [2, 17, 18]. As a consequence of the chemical interaction between the NO_2 molecules and the resultant adsorption on the carbon film surface which causes electrical charge to be transferred between them and hence changes the carrier concentration, the channel conductivity varies during the process [19, 20].

In the other hand the conductance characteristic will increase when the gas molecule adsorption occurred on the surface of carbon Theoretical studies have confirmed the remarkable change in electronic properties of carbon film due to the detection of gas molecules. Most molecules are known to be an electron-acceptor such as NO_2 and O_2 or an electron donor such as NH_3 and H_2O displaying relatively small charge transfer between adsorbed molecules weakly on the carbon film wall [21-24]. carbon films show p-type semiconducting property of decreasing resistance upon exposure of NO_2 gas [25-27]. To produce the analytical investigation the curve fitting of MATLAB software was used. The obtained formula is shown in Equation (1).

$$F(x) = a\exp(bx) + c\exp(dx) \quad (1)$$

The parameters a, b, c, and d are constants and the regression values are listed in Table 4.

Table 4. Values for a, b, c, d parameters and the corresponding regressions

Equation	Gas	Gas exposure	a	B	C	d	R
$F(x) = a\exp(bx) + c\exp(dx)$	CO2	Without gas	-7.043e+5	-0.1136	7.043e+5	-0.1136	0.9968
		200 ppm	6.861e+5	-0.1312	-6.861e+5	-0.1312	0.9985
		400 ppm	81.59	0.00037	-80.3	-0.5398	0.9998
		800 ppm	74.3	0.05355	-74.98	-1.246	0.9994
	NO2	Without gas	-4.884e+06	-0.161	4.884e+06	-0.161	0.9979
		200 ppm	8.859e+05	-0.1607	-8.859e+05	-0.1608	0.9989
		400 ppm	56.48	0.05094	-70.78	-0.7854	0.9992
		800 ppm	76.06	0.03812	-95.23	-0.848	0.9991

4. Conclusion

The current-voltage characteristics of the obtained C-strands were tested and evaluated before and after exposure to three gases, Methane, CO_2 and NO_2 in order to assess their potential ability to replace the channel in gas sensors. While applying a DC voltage to the C-strands in successive time periods after the growth, the corresponding currents passing through the conductive channel has been measured and recorded. Two main observations were made during the experimental study. Firstly, the electrode configuration and the gaps between them have direct impact on the fineness and the conductivity of the carbonaceous material. Secondly, the conductivity of the C-strand changes in the presence of gas, i.e. when the channel is exposed to gas, due to the adsorption of gas atoms on the surface of the C-strand, its conductivity increases. Therefore, as a general conclusion, this study proposes that C-strand material can be used in gas detection sensors presenting high sensitivity and empowering the sensor manufacturers to produce accurate sensing mechanisms in extremely smaller sizes.

Acknowledgments

The authors would like to thank the Ministry of Education (MOE), Malaysia (grant Vot. No. 4F382) and the Universiti Teknologi Malaysia (GUP grant Vot. No. 07H56 and Post-Doc grant Vot. No. 02E87) for the financial support received during the investigation.

References

[1] E Akbari *et al*. Analytical Calculation of Sensing Parameters on Carbon Nanotube Based Gas Sensors. *Sensors.* 2014; 14(3): 5502-5515.
[2] L Valentini, I Armentano, J Kenny, C Cantalini, L Lozzi, S Santucci. Sensors for sub-ppm NO 2 gas detection based on carbon nanotube thin films. *Applied Physics Letters.* 2003; 82(6): 961-963.
[3] Y. Battie *et al.*. Gas sensors based on thick films of semi-conducting single walled carbon nanotubes. *Carbon.* 2011; 49(11): 3544-3552.
[4] JJ Adjizian *et al.* Boron-and nitrogen-doped multi-wall carbon nanotubes for gas detection. *Carbon.* 2014; 66: 662-673.
[5] RM Balabin, EI Lomakina. Support vector machine regression (LS-SVM)—an alternative to artificial neural networks (ANNs) for the analysis of quantum chemistry data?. *Physical Chemistry Chemical Physics.* 2011; 13(24): 11710-11718.
[6] SMZ Iqbal. Decomposition of Methane Into Carbonaceous Material Using Arc Discharge Method. PhD, Electrical Power, IUniversiti Teknologi Malaysia, Malaysia, 2014.
[7] N Muradov. Catalysis of methane decomposition over elemental carbon. *Catalysis communications.* 2001; 2(3): 89-94.
[8] F Krcma, K Klohnova, L Polachova, G Horvath. Optical Emission Spectroscopy Of Abnormal Glow Discharge In Nitrogen-Methane Mixtures At Atmospheric Pressure. *Publications de l'Observatoire Astronomique de Beograd.* 2010; 89: 371-374.
[9] C PATACSIL, G MALAPIT, H RAMOS. Optical Emission Spectroscopy of Low Temperature CVD Diamond. *J Plasma Fusion Res Ser.* 2006; 7: 145-149.
[10] L Vanajakshi, LR Rilett. A comparison of the performance of artificial neural networks and support vector machines for the prediction of traffic speed. in *Intelligent Vehicles Symposium, 2004 IEEE*, 2004: 194-199.

[11] C Fantini, A Jorio, M Souza, M Strano, M Dresselhaus, M Pimenta. Optical transition energies for carbon nanotubes from resonant Raman spectroscopy: Environment and temperature effects. *Physical review letters.* 2004; 93(14): 147406.
[12] CM Bishop, *Pattern recognition and machine learning*. springer New York, 2006.
[13] YK Moon, J Lee, JK Lee, TK Kim, SH Kim. Synthesis of Length-Controlled Aerosol Carbon Nanotubes and Their Dispersion Stability in Aqueous Solution. *Langmuir.* 2009; 25(3): 1739-1743.
[14] E K Lee *et al.* Catalytic decomposition of methane over carbon blacks for CO2-free hydrogen production. *Carbon.* 2004; 42(12–13): 2641-2648.
[15] J Zhang, L Jin, Y Li, H Si, B Qiu, H Hu. Hierarchical porous carbon catalyst for simultaneous preparation of hydrogen and fibrous carbon by catalytic methane decomposition. *International Journal of Hydrogen Energy.* 2013; 38(21): 8732-8740.
[16] RF N Patel, N Bazzanella, A Miotello. Enhanced hydrogen production by hydrolysis of NaBH4 using —C◆B nanoparticles supported on Carbon film" catalyst synthesized by pulsed laser deposition. *Elsevier.* 2011; 170(1): 20–26.
[17] HJ Park *et al*. Highly flexible, mechanically stable, and sensitive NO2 gas sensors based on reduced graphene oxide nanofibrous mesh fabric for flexible electronics. *Sensors and Actuators B: Chemical.* 2018; 257: 846-852.
[18] I Hotovy, V Rehacek, P Siciliano, S Capone, L Spiess. Sensing characteristics of NiO thin films as NO2 gas sensor. *Thin Solid Films.* 2002; 418(1): 9-15.
[19] Z Su *et al.* Cu-modified carbon spheres/reduced graphene oxide as a high sensitivity of gas sensor for NO 2 detection at room temperature. *Chemical Physics Letter.* 2018.
[20] ST Shishiyanu, TS Shishiyanu, OI Lupan. Novel NO2 gas sensor based on cuprous oxide thin films. *Sensors and Actuators B: Chemical.* 2006; 113(1): 468-476.
[21] RL van Ewyk, AV Chadwick, JD Wright. Electron donor–acceptor interactions and surface semiconductivity in molecular crystals as a function of ambient gas. *Journal of the Chemical Society, Faraday Transactions 1: Physical Chemistry in Condensed Phases.* 1980; 76: 2194-2205.
[22] L Bai, Z Zhou. Computational study of B-or N-doped single-walled carbon nanotubes as NH3 and NO2 sensors. *Carbon.* 2007; 45(10): 2105-2110.
[23] C Jamorski, JB Foresman, C Thilgen, HP Lüthi. Assessment of time-dependent density-functional theory for the calculation of critical features in the absorption spectra of a series of aromatic donor–acceptor systems. *The Journal of chemical physics.* 2002; 116(20): 8761-8771.
[24] Y Cheng, R Meng, C Tan, X Chen, J Xiao. Selective gas adsorption and I–V response of monolayer boron phosphide introduced by dopants: A first-principle study. *Applied Surface Science.* 2018; 427: 176-188.
[25] J Suehiro, G Zhou, H Imakiire, W Ding, M Hara. Controlled fabrication of carbon nanotube NO2 gas sensor using dielectrophoretic impedance measurement. *Sensors and Actuators B: Chemical.* 2005; 108(1-2): 398-403.
[26] W Shi, J Yu, HE Katz. Sensitive and selective pentacene-guanine field-effect transistor sensing of nitrogen dioxide and interferent vapor analytes. *Sensors and Actuators B: Chemical.* 2018; 254: 940-948.
[27] Z Maniei, E Shakerzadeh, Z Mahdavifar. Theoretical approach into potential possibility of efficient NO2 detection via B40 and Li@ B40 fullerenes. *Chemical Physics Letters.* 2018; 691: 360-365.